Microfluidic on-chip Production of Alginate Hydrogels Using Double Co-flow Geometry

Amirmohammad Sattari
University of Tehran
Sajad Janfaza
University of British Columbia
Mohsen Mashhadi Keshtiban
University of Tehran
Nishat Tasnim
University of British Columbia
Pedram Hanafizadeh
University of Tehran
Mina Hoorfar (mina.hoorfar@ubc.ca)
University of British Columbia

Research Article

Keywords: Microfluidic on-chip, Alginate Hydrogels, microgels

Posted Date: April 22nd, 2021

DOI: https://doi.org/10.21203/rs.3.rs-439280/v1

Abstract

Microfluidic on-chip production of microgels employing external gelation has numerous biological and pharmaceutical applications, particularly for the encapsulation of delicate cargos, however, the on-chip production of microgels in microfluidic devices can be challenging due to problems such as clogging caused by accelerated progress in precursor solution viscosity. Here, we introduce a novel microfluidic design incorporating two consecutive co-flow geometries for microfluidic droplet generation. A shielding oil phase is employed to avoid emulsification and gelation stages from occurring simultaneously, thereby preventing clogging. The results revealed that the microfluidic device could generate highly monodispersed spherical droplets (coefficient of variation < 3%) with an average diameter in the range of 60–200 μm. Additionally, it was demonstrated that the device could appropriately create a shelter of the oil phase around the inner aqueous phase regardless of the droplet formation regime and flow conditions. The ability of the proposed microfluidic device in the generation of microgels was validated by producing alginate microgels utilizing an aqueous solution of calcium chloride as the continuous phase.

Introduction

There has been a thriving interest in microfluidics due to their breadth of applications in diverse branches of science and industry, from biological applications to food science and chemistry. By operating at a miniature scale, microfluidic systems can offer advantages such as regulating and manipulating fluids with tremendous precision, enabling precise control over small sample volumes, and reducing analysis time [1]. Attention to the droplet-based microfluidic systems has been expanding extensively in past decades due to their substantial applications in various areas, such as cell culture [2], chemical synthesis [3], extraction and phase transfer [4], etc.

The production of emulsions and microparticles employing microfluidic platforms has gained noteworthy attention in recent years due to their significant benefits over traditional bulk methods [5]. In the so-called bulk methods, such as precipitation polymerization and emulsion polymerization, there is minimal control over particles monodispersity, uniformity of crosslink density, and morphology, especially for creating complex geometries such as multiple emulsions [6]. In contrast, droplet-based microfluidics systems facilitate practical and precise control in the fabrication of microparticles and emulsions [7]. Monodispersed microdroplets generated in microfluidic platforms can provide a compartment in which reactions or species can be separated from the surrounding environment, so it is fitting for quantitative investigations on cell analysis applications and suggests a meaningful number of opportunities in biological and chemical applications [8]. Furthermore, droplet-based microfluidics technology allows the generation of monodispersed and shape-controlled microgels, which has numerous applications in cell biology [9], tissue engineering [10], drug delivery [11], and separation processes [12].

The microfluidic production of the microgels typically consists of two steps, including microfluidic emulsification of forerunner solutions and gelation of the produced droplets, which can be done in either

on-chip or off-chip mode. The on-chip gelation method is commonly favored since it has numerous advantages over off-chip gelation, including simplified manipulation of the microgels' morphologies, facilitated way for loading a wide diversity of cargos, and continuous production of the microgels with an extraordinary degree of monodispersity [13], [14]. Yet, there are several outstanding challenges with the on-chip gelation method, one major factor being the immediate development of the cross-linking process, which may result in the occlusion of the microchannels and/or inlets and outlets. The production of microgel with controlled morphology and dispersity also requires the inclusion of a time lag between the emulsification and gelation processes [14]. Several research groups have come up with some innovative ideas to solve this issue. One novel idea, first proposed by Wang et al. [15], took advantage of a blocking stream to prevent premature gelation. In their study, a water stream was incorporated in the middle microchannel to inhibit the mixing of ionic triblock copolymers with a separate charge, which moves in the side microchannels prior to the flow-focusing nozzle. Similar work was presented by Mazutis et al. [16], employing a two consecutive flow-focusing configuration. They passed a water flow stream from the central channel, which prevented the immature generation of alginate microgels from cross-linking with the calcium chloride solution.

Microfluidic preparation of precursor solutions can be fundamentally classified into two approaches: channel-based microfluidics and planner surface approach [17]. In the so-called channel-based systems, the interaction among continuous and dispersed phases causes the breakup and generation of single droplets. In contrast, in the planner surface technique, or as regularly called digital microfluidics, from an actuation mechanism through electrowetting or dielectrophoresis techniques, the breakup happens [18]. There are some conventional geometries to generate droplets in microfluidic systems, named T-junction [19], flow-focusing [20], co-flowing [21], membrane [22], and step emulsification [23], which are classified in channel-based microfluidics. As a general comparison between mentioned emulsification methods, membrane structures provide the highest throughput, while they suffer from a relatively poor monodispersity [24]. From another point of view, among the mentioned structures, co-flow geometry requires a minimum surface treatment procedure because the core fluid stream remains enclosed within the continuous stream during droplet formation [25]. Hence, the inner jet stream does not touch the microchannel wall, and therefore no surface wall treatment is required for the production of microdroplets. This configuration also benefits from high monodispersity and significant throughput of droplet generation compared to other conventional geometries [1]. Various combinations of the aforementioned geometries have been widely used due to take advantage of both geometry [26] and generation of double emulsions [27] such as two subsequent T-junctions [28], flow-focusing [29], and co-flowing [30], a combination of T-junction and co-flowing [31], and a combination of T-junction and flow-focusing [32]. As discussed earlier, on-chip gelation of microdroplets still remained a challenging technique due to the need to precisely control the gelation process within the microchannel, which requires to be studied more.

In this study, we developed a novel microfluidic device for the generation of highly monodispersed spherical microgels using double co-flow geometry. Our proposed design included the features of facile emulsification and controllable gelation to mitigate challenges with the microfluidic production of

microgels. Concerning the emulsification process, we employ a double co-flow geometry comprised of the two same-level high aspect ratio co-flow channels introduced in our previous study [25]. In the proposed double co-flow geometry, a shielding oil phase is utilized to extend the crosslinking process to the end of the microchannel at the outlet to have highly monodispersed and spherical droplets. We have also examined the effects of all three phase flow rates on the diameter and size distribution of microdroplets. Besides, an off-chip evaluation of the shape and size of microgels revealed a succeeding gelation process in the proposed microfluidic device.

Materials And Methods

Materials

The inner phase consisted of 1.5% (wt) Sodium alginate (19–40 kDa) dispersed in deionized water. The shielding phase consisted of a mixture of 0.3% (w/w) Span 80 in light mineral oil (Sigma-Aldrich). The crosslinking phase comprised an emulsion of calcium chloride aqueous solution as a crosslinking agent with two different concentrations of 0.1 and 1 mol/L. All experiments were conducted at room temperature (20°C) and atmospheric conditions (1 bar).

Geometric Model

The proposed geometry comprises three distinct rectangular microchannels with the same axis, which is shown in Fig. 1a. All three internal channels have a width of 40 μm, while the outer channels close to the side walls have a 60 μm width, and the microfluidic chip has a constant height of 120 μm. The inner phase is introduced through the central channel, while the intermediate shielding phase is injected from its two side channels. The crosslinking phase also flows from the outermost channels. The total length of the main channel is about 5000 μm, which is sufficient for diminishing the effects of the outlet on the droplet formation. All inlets and outlets are circular in shape with an average diameter of 1100 μm.

The shape of the fabricated mold, particularly at the junctions, was assessed with the use of a surface profilometer (Profilm3D, Filmetrics). A view of the probe passing along the fabricated mold is presented in Fig. 1b. The profile of the silicone-SU-8 mold showed a satisfactory depth and proper space between walls (Fig. 1c).

Microfabrication

The PDMS channel was produced in the cleanroom using a SU-8 mold fabricated on a silicon substrate. SU-8 2075 (MicroChem Corp) was spin-coated on a 3 inches silicon wafer considering the guideline provided by MicroChem to achieve 120 μm mold height. The silicon wafer was soft-baked at 65℃ and 95℃ for 3 and 5 minutes, respectively. It was then exposed to the Ultraviolet (UV) light and is proceeding under Post-Exposure-Bake (PEB) at 95℃ for 5 minutes. Instantly, the silicon wafer was immersed in the SU-8 developer for about 8 minutes and patterned. After wiping with isopropanol, the mold was hard-baked for almost 30 minutes at 150 ℃.

A proper amount of PDMS and its curing agent (Dow Corning) are mixed with a 10:1 ratio and poured over the mold. Following the elimination of bubbles in a desiccator and curing in the oven at 70℃ for about five hours, the PDMS channel was peeled off, and the inlets and outlets were punched using a 1 mm puncher. Ultimately, the PDMS and glass surfaces are treated in an oxygen plasma chamber and are bonded immediately.

On-Chip Gelation

In order to generate alginate microgels, the inner aqueous phase containing 1.5% w/w of alginate in DI water was inserted from the central channel, and the shelter phase containing 0.3% w/w Span 80 in light mineral oil was injected through the side channels. The mineral oil acted as the continuous phase for the generation of alginate microdroplets as well as a shelter phase to prevent the immediate development of the cross-linking process. The crosslinking phase consisted of an aqueous solution of calcium chloride with two various concentrations of 0.1 and 1 mol L^{-1}, which was flowed through the outermost channels.

In the proposed configuration, alginate microdroplets remained enclosed by the shelter phase up to the end of the main channel. At the outlet, which functioned as a step due to a greater height compared to the other parts of the microchannel, the shelter phase ruptured, resulting in the penetration of the crosslinking phase to the alginate microdroplets, creating microgels at the outlet of the device. The produced microgels then left the device through a silicone tube and were collected in microtubes. It should be noted that using the proper concentration of calcium chloride in the crosslinking phase (more than 1 mol L^{-1}), leads to highly monodispersed and spherical droplets due to the prevention from the cross-linking process through the channel and gelation process right at the outlet.

Experimental Setup and Image Analysis

The setup includes a biological microscope (Zeiss Company, Germany), a high-speed video camera (XIMEA Company, Germany), three automatic syringe pumps (SAMA Instruments) for relatively constant flow infusion to the microfluidic channels, the microfabricated PDMS chip, a computer for collecting videos and controlling the syringe pumps, and a reservoir for collecting generated microgels. Videos were obtained at a frequency rate of 2000 Hz and were analyzed using Droplet Morphometry and Velocimetry (DMV) Matlab-based software [33].

Results And Discussion

We have investigated the influence of phase flow rates on the overall diameter and size distribution of microdroplets in dual co-flow geometry, with the presence of shielding oil phase. Also, we have studied the effects of outer phase flow rate and calcium chloride concentration on the roundness and size distribution of produced microgels.

Overall Observation

The formation of alginate droplets shielding by the middle oil phase from the continuous crosslinking phase in various flow conditions is depicted in Fig. 2. In all flow conditions, the middle oil phase prevents the inner alginate droplets from crosslinking with the continuous phase along the microchannel. At the end of the main channel, the middle oil phase ruptures, and the crosslinking process begins. Note that because of the presence of the silicone tube at the outlet of the channel, the direct observation of the mentioned happenings was not possible. Nevertheless, the off-chip observation of cross-linked alginate droplets showed the commencement of crosslinking at the outlet of the designed microchip.

As a general observation, increasing the continuous phase flow rate results in smaller alginate droplets and a narrower shielding phase jet (Fig. 2a & b). Similarly, an increment in the flow rate of the middle phase leads to the smaller alginate droplets due to the higher shear rate imposed by the middle oil phase. However, the higher momentum of the shielding jet overcomes the shear rate acted upon by the crosslinking phase to its interface and results in a wider shielding jet stream (Fig. 2a & c). Finally, the inner phase flow rate growth results in the transition from dripping to the jetting regime. This leads to both larger droplets and wider middle phase jet stream because the shielding jet is blocked by the forming jet of the inner alginate stream (Fig. 2a & d).

Effect of outer phase flow rate

The influence of crosslinking phase flow rate on the alginate droplets' equivalent diameter and size distribution is demonstrated in Fig. 3. As seen in the figure, the increment of the continuous phase flow rate resulted in smaller alginate droplets. The decrease in the inner droplet diameter is principally due to increased shear stress implemented by the continuous phase stream to the shielding phase jet interface. Increasing the outer phase velocity manages the suppression of the oil phase jet, which also diminishes the formation time and tends to the formation of smaller alginate droplets.

Of note, higher crosslinking phase flow rates lead to the higher polydispersity of the size of alginate droplets, i.e., the coefficient of variation is larger in the condition of the higher shear rate imposed to the forming jet of the inner phase. This can be justified by the fact that the higher shear rates imposed by the continuous phase result in the shielding phase jet stream moving away from a symmetrical shape due to the higher instabilities on the shielding jet interface. This creates a disturbance in the formation of alginate droplets leading to the lower monodispersity of droplets.

Effect of shielding phase flow rate

The effects of middle phase flow rate on the alginate droplets' equivalent diameter and size distribution are demonstrated in Fig. 4. As shown, the increment of the shielding phase flow rate results in smaller alginate droplets and transition from jetting to dripping regimes. Also, the middle phase jet gets wider whatever the middle phase flow rate increases, and also fewer numbers of instabilities can be seen. The decrease in the inner droplet diameter is essentially due to the larger shear stress implemented by the oil phase stream to the inner droplet interface. Thus, it manages the suppression of the alginate phase jet, leading it to the dripping regime and causing the formation of smaller droplets. Furthermore, the size distribution of microdroplets is much narrower in the dripping regime (higher flow rates of middle oil

phase), and therefore alginate droplets had higher monodispersity than in lower flow rates of the middle phase and jetting regime.

Effect of alginate phase flow rate

The increment of inner phase flow rate led to the transition from the dripping to the jetting regimes and also the formation of larger alginate droplets, as shown in Fig. 5. An increase in innermost phase velocity leads to a growth in the inner phase droplet diameter. The growth in droplet diameter occurs as a result of the increase in both inertial and viscous forces of the internal phase, which indicates more surface tension force is expected to dominate inertia and viscous forces for the breakup process that is achieved by larger droplets in constant surface tension states. Furthermore, due to the transition from dripping to the jetting regime at higher inner phase flow rates, the monodispersity diminishes as the inner phase flow rate increases.

Of-chip investigation of alginate microgels

We have also investigated the effect of calcium chloride concentration in the crosslinking phase emulsion on the capability of synthesis of microgels. In order to analyze this parameter, the concentration of calcium chloride was considered 0.1 and 1 mol/L. In low calcium chloride concentrations, non-spherical microgels with a drop-like shape (also called the teardrop or tail-shaped) were produced (Fig. 6a & b). The production of teardrop-shaped microgels indicated that complete gelation process or most of it occurred outside of the microfluidic device in the outlet tube [14], [34]. An observation that verifies this theory is the formation of spherical alginate droplets during our experiments. As shown in Fig. 2, the generated alginate droplets were quite spherical, and if their gelation process happened solely in the microfluidic device, the produced microgels should be spherical as well. Even if the gelation process happens partly (just a shell forms around the alginate droplets), provided that this shell has a sufficient thickness, it can sustain the spherical shape of microgels after leaving the microfluidic chip [35].

As represented in Fig. 6c & d, the shape of produced microgels became more spherical by increasing calcium chloride concentration. This observation confirms that at higher concentrations of calcium chloride, a greater portion of the gelation process happens inside the microfluidic device, and consequently, microgel production shifts to a more on-chip process. This remark is presumably due to the quicker diffusion of more calcium ions from crosslinking phase into the alginate droplets at higher calcium chloride concentrations. Thus, this will cause faster gelation of alginate droplets, leading to on-chip gelation of these droplets and sustaining their spherical shape after gelation.

We examined the influence of the outer phase flow rate on the gelation process, as depicted in Fig. 6. As discussed previously, the increment in the external phase flow rate leads to the smaller alginate droplets. Consequently, smaller crosslinked droplets can be seen in both concentrations (Fig. 6b & d compared to Fig. 6a & c). We observed that the roundness of droplets' shape was slightly greater in higher flow rates of the outer phase than the lower flow rates. This indicated that a more significant portion of the gelation process occurred inside the microfluidic device, and microgel generation shifts to an on-chip process. That was predictable since the crosslinking phase flow rate increment leads to a narrower intermediate

shielding phase; consequently, the penetration of the crosslinking phase into the alginate microdroplets is more readily compared to the broader middle phase jet stream conditions, and most of the gelation process occurred on-chip.

Effect of outer phase flow rate and calcium chloride concentration on characteristics of microgels

The quantitative measurement of roundness and coefficient of variation in various outer phase flow rates and two distinct concentrations of calcium chloride was performed and shown in Fig. 7. The increment in the outer phase flow rate leads to the lower monodispersed droplets, i.e., a higher coefficient of variation. The decreased in monodispersity can be attributed to higher shear rates in the continuous phase resulting in a more asymmetrical shape of the shielding phase. Consequently, more disturbances affecting the formation of alginate microdroplets, resulting in the lower monodispersity of droplets. Nevertheless, the coefficient of variation of droplet sizes remained under 3% for the worst condition (the highest flow rate of the crosslinking phase), which shows the capability of our proposed device to generate highly monodispersed droplets.

Besides, higher flow rates of the crosslinking phase result in more spherical alginate microgels, and this sphericality enhances more as the concentration of the calcium chloride increases in the crosslinking phase. Generally speaking, the roundness of alginate droplets is not acceptable in low concentrations of calcium chloride at low flow rates of the crosslinking phase ($Q0 < 2000$ µl / hr). In contrast, the roundness is quite acceptable in all conditions of the crosslinking phase flow rate for 1 mol/L calcium chloride concentration (roundness is more than 0.85 in all situations).

Conclusion

In this study, the microfluidic on-chip generation of alginate microgels using an external gelation method was accomplished by employing a double co-flow configuration. A sheltered oil phase was utilized for alginate droplet shielding, which prevents the process of emulsification and gelation from taking place simultaneously. The effects of phase flow rates on the droplet characteristics, including equivalent diameter and coefficient of variation, were examined. The ability of the proposed device to produce highly monodispersed spherical microgels was confirmed by creating alginate microgels through external gelation of alginate droplets shielded by the mineral oil phase with calcium chloride continuous phase at the outlet of the device. Moreover, the impact of calcium chloride concentration in the crosslinking phase on the gelation process was investigated. Overall, the experiment results confirmed the ability of double co-flow geometry in the production of highly monodispersed spherical microgels. The proposed design is particularly applicable for microfluidic encapsulation of sensitive loads using microgels due to the adopted shielding phenomenon and on-chip external gelation method.

Declarations

Amirmohammad Sattari: Conceptualization, Data curation, Formal Analysis, Investigation, Methodology, Writing – original draft.

Sajad Janfaza: Data curation, Investigation, Methodology.

Mohsen Mashhadi Keshtiban: Data curation, Formal Analysis, Methodology, Validation, Writing – review & editing.

Nishat Tasnim: Writing – review & editing, Methodology, Formal Analysis.

Pedram Hanafizadeh: Conceptualization, Investigation, Project administration, Supervision, Writing – review & editing.

Mina Hoorfar: Conceptualization, Investigation, Project administration, Supervision, Writing – review & editing.

Additional Information

There are no conflicts to declare.

References

[1] A. Sattari, P. Hanafizadeh, and M. Hoorfar, “Multiphase flow in microfluidics: From droplets and bubbles to the encapsulated structures,” *Adv. Colloid Interface Sci.*, vol. 282, 2020, doi: 10.1016/j.cis.2020.102208.

[2] H. N. Joensson and H. Andersson Svahn, “Droplet microfluidics—A tool for single-cell analysis,” *Angew. Chemie Int. Ed.*, vol. 51, no. 49, pp. 12176–12192, 2012.

[3] K. S. Elvira, X. C. i Solvas, R. C. R. Wootton, and A. J. Demello, “The past, present and potential for microfluidic reactor technology in chemical synthesis,” *Nat. Chem.*, vol. 5, no. 11, p. 905, 2013.

[4] C. E. Poulsen, R. C. R. Wootton, A. Wolff, A. J. deMello, and K. S. Elvira, “A microfluidic platform for the rapid determination of distribution coefficients by gravity-assisted droplet-based liquid–liquid extraction,” *Anal. Chem.*, vol. 87, no. 12, pp. 6265–6270, 2015.

[5] S. Y. Teh, R. Lin, L. H. Hung, and A. P. Lee, “Droplet microfluidics,” *Lab Chip*, vol. 8, no. 2, pp. 198–220, 2008, doi: 10.1039/b715524g.

[6] W. Li *et al.*, “Microfluidic fabrication of microparticles for biomedical applications,” *Chem. Soc. Rev.*, vol. 47, no. 15, pp. 5646–5683, 2018, doi: 10.1039/c7cs00263g.

[7] R. Seemann, M. Brinkmann, T. Pfohl, and S. Herminghaus, “Droplet based microfluidics,” *Reports Prog. Phys.*, 2012, doi: 10.1088/0034-4885/75/1/016601.

[8] A. B. Theberge *et al.*, “Microdroplets in microfluidics: An evolving platform for discoveries in chemistry and biology,” *Angewandte Chemie - International Edition*. 2010, doi: 10.1002/anie.200906653.

[9] S. Girardo *et al.*, “Standardized microgel beads as elastic cell mechanical probes,” *J. Mater. Chem. B*, 2018, doi: 10.1039/c8tb01421c.

[10] E. Guermani *et al.*, “Engineering complex tissue-like microgel arrays for evaluating stem cell differentiation,” *Sci. Rep.*, 2016, doi: 10.1038/srep30445.

[11] C. X. Zhao, “Multiphase flow microfluidics for the production of single or multiple emulsions for drug delivery,” *Adv. Drug Deliv. Rev.*, vol. 65, no. 11–12, pp. 1420–1446, 2013, doi: 10.1016/j.addr.2013.05.009.

[12] D. Dendukuri and P. S. Doyle, “The synthesis and assembly of polymeric microparticles using microfluidics,” *Adv. Mater.*, 2009, doi: 10.1002/adma.200803386.

[13] E. Tumarkin and E. Kumacheva, “Microfluidic generation of microgels from synthetic and natural polymers,” *Chem. Soc. Rev.*, vol. 38, no. 8, pp. 2161–2168, 2009.

[14] H. Shieh, M. Saadatmand, M. Eskandari, and D. Bastani, “Microfluidic on-chip production of microgels using combined geometries,” *Sci. Rep.*, 2021, doi: 10.1038/s41598-021-81214-7.

[15] C. X. Wang, S. Utech, J. D. Gopez, M. F. J. Mabesoone, C. J. Hawker, and D. Klinger, “Non-Covalent Microgel Particles Containing Functional Payloads: Coacervation of PEG-Based Triblocks via Microfluidics,” *ACS Appl. Mater. Interfaces*, 2016, doi: 10.1021/acsami.6b03356.

[16] L. Mazutis, R. Vasiliauskas, and D. A. Weitz, “Microfluidic Production of Alginate Hydrogel Particles for Antibody Encapsulation and Release,” *Macromol. Biosci.*, 2015, doi: 10.1002/mabi.201500226.

[17] S. Mashaghi, A. Abbaspourrad, D. A. Weitz, and A. M. van Oijen, “Droplet microfluidics: A tool for biology, chemistry and nanotechnology,” *TrAC Trends Anal. Chem.*, vol. 82, pp. 118–125, 2016.

[18] S. Haeberle and R. Zengerle, “Microfluidic platforms for lab-on-a-chip applications,” *Lab Chip*, vol. 7, no. 9, pp. 1094–1110, 2007.

[19] T. Fu, Y. Ma, D. Funfschilling, C. Zhu, and H. Z. Li, “Squeezing-to-dripping transition for bubble formation in a microfluidic T-junction,” *Chem. Eng. Sci.*, vol. 65, no. 12, pp. 3739–3748, 2010.

[20] S. L. Anna, N. Bontoux, and H. A. Stone, “Formation of dispersions using ‘flow focusing’ in microchannels,” *Appl. Phys. Lett.*, vol. 82, no. 3, pp. 364–366, 2003, doi: 10.1063/1.1537519.

[21] A. S. Utada, A. Fernandez-Nieves, H. A. Stone, and D. A. Weitz, “Dripping to jetting transitions in coflowing liquid streams,” *Phys. Rev. Lett.*, vol. 99, no. 9, p. 94502, 2007.

[22] D. Vanswaay, T. Y. D. Tang, S. Mann, and A. DeMello, “Microfluidic Formation of Membrane-Free Aqueous Coacervate Droplets in Water,” *Angew. Chemie - Int. Ed.*, vol. 54, no. 29, pp. 8398–8401, 2015,

doi: 10.1002/anie.201502886.

[23] M. L. Eggersdorfer, H. Seybold, A. Ofner, D. A. Weitz, and A. R. Studart, “Wetting controls of droplet formation in step emulsification,” *Proc. Natl. Acad. Sci. U. S. A.*, 2018, doi: 10.1073/pnas.1803644115.

[24] A. J. Abrahamse, A. der Padt, R. M. Boom, and W. B. C. De Heij, “Process fundamentals of membrane emulsification: simulation with CFD,” *AIChE J.*, vol. 47, no. 6, pp. 1285–1291, 2001.

[25] A. Sattari and P. Hanafizadeh, “Controlled preparation of compound droplets in a double rectangular co-flowing microfluidic device,” *Colloids Surfaces A Physicochem. Eng. Asp.*, vol. 602, no. February, p. 125077, 2020, doi: 10.1016/j.colsurfa.2020.125077.

[26] C. Priest, S. Herminghaus, and R. Seemann, “Generation of monodisperse gel emulsions in a microfluidic device,” *Appl. Phys. Lett.*, 2006, doi: 10.1063/1.2164393.

[27] D. T. Chong *et al.*, “Advances in fabricating double-emulsion droplets and their biomedical applications,” *Microfluidics and Nanofluidics*. 2015, doi: 10.1007/s10404-015-1635-8.

[28] B. Thompson, C. T. Riche, N. Movsesian, K. C. Bhargava, M. Gupta, and N. Malmstadt, “Engineered hydrophobicity of discrete microfluidic elements for double emulsion generation,” *Microfluid. Nanofluidics*, vol. 20, no. 5, p. 78, 2016.

[29] C. Y. Liao and Y. C. Su, “Formation of biodegradable microcapsules utilizing 3D, selectively surface-modified PDMS microfluidic devices,” *Biomed. Microdevices*, 2010, doi: 10.1007/s10544-009-9367-8.

[30] A. Perro, C. Nicolet, J. Angly, S. Lecommandoux, J. F. Le Meins, and A. Colin, “Mastering a double emulsion in a simple co-flow microfluidic to generate complex polymersomes,” *Langmuir*, 2011, doi: 10.1021/la1037102.

[31] S. Huang, S. Zeng, Z. He, and B. Lin, “Water-actuated microcapsules fabricated by microfluidics,” *Lab Chip*, vol. 11, no. 20, pp. 3407–3410, 2011.

[32] C. N. Lim, K. S. Koh, Y. Ren, J. K. Chin, Y. Shi, and Y. Yan, “Analysis of liquid-liquid droplets fission and encapsulation in single/two layer microfluidic devices fabricated by xurographic method,” *Micromachines*, vol. 8, no. 2, 2017, doi: 10.3390/mi8020049.

[33] A. S. Basu, “Droplet morphometry and velocimetry (DMV): A video processing software for time-resolved, label-free tracking of droplet parameters,” *Lab Chip*, vol. 13, no. 10, pp. 1892–1901, 2013, doi: 10.1039/c3lc50074h.

[34] C. Kim *et al.*, “Rapid exchange of oil-phase in microencapsulation chip to enhance cell viability,” *Lab Chip*, 2009, doi: 10.1039/b819044e.

[35] M. Samandari, F. Alipanah, S. H. Javanmard, and A. Sanati-Nezhad, “One-step wettability patterning of PDMS microchannels for generation of monodisperse alginate microbeads by in Situ external gelation in double emulsion microdroplets,” *Sensors Actuators B Chem.*, vol. 291, pp. 418–425, 2019.

Figures

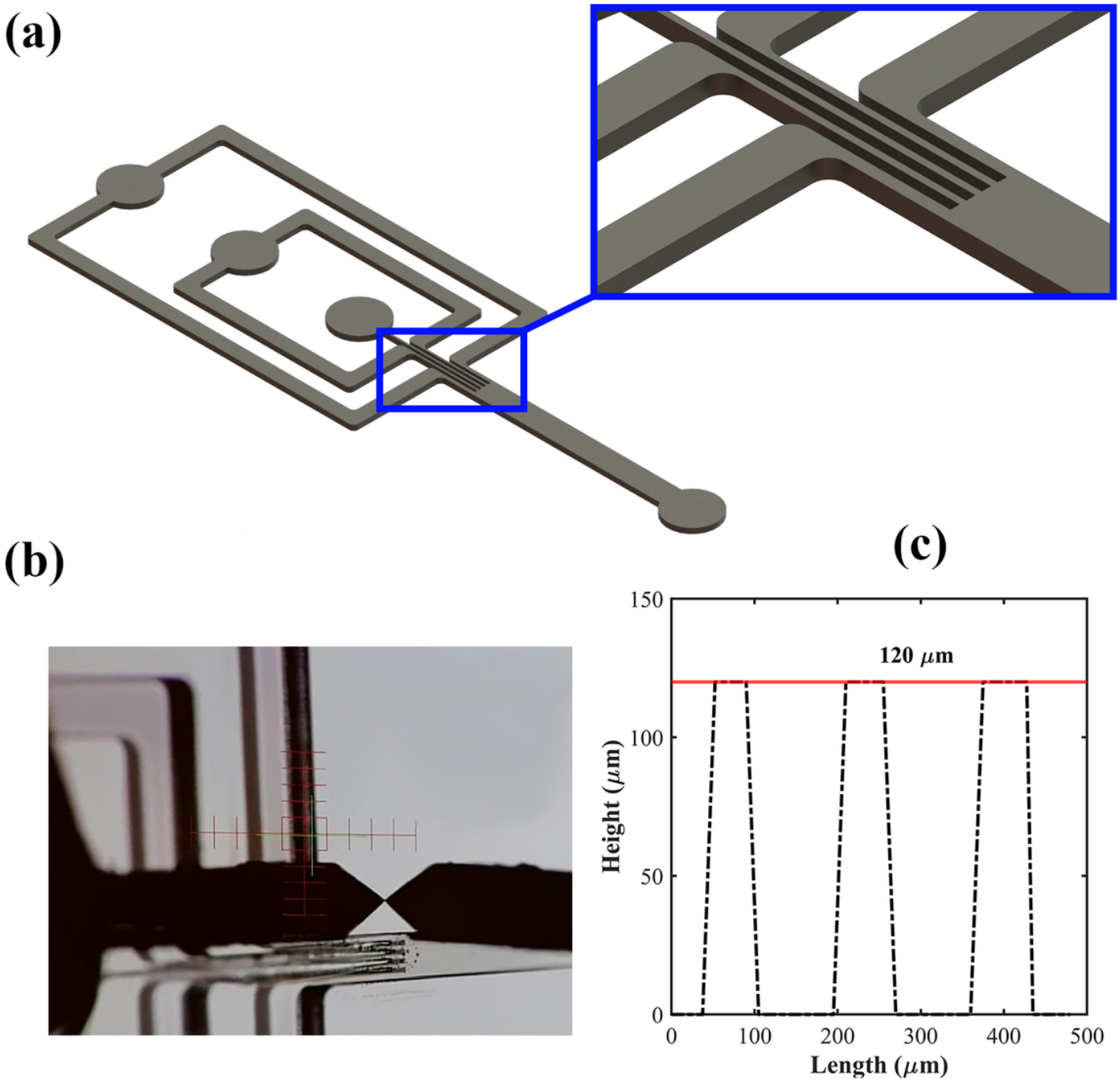

Figure 1

(a) Three-dimensional view of the designed double co-flow geometry, (b) an image of the surface profilometer device, and (c) results of the profile obtained from the surface profilometry.

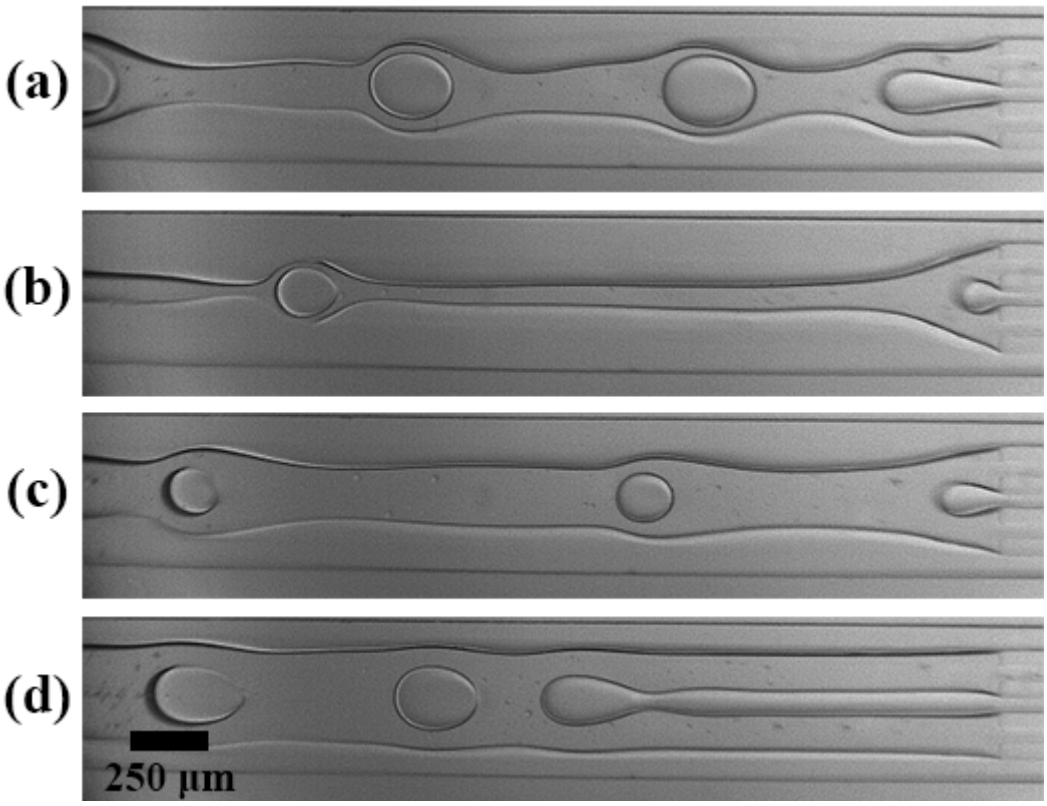

Figure 2

Please see the Manuscript file for the complete figure caption.

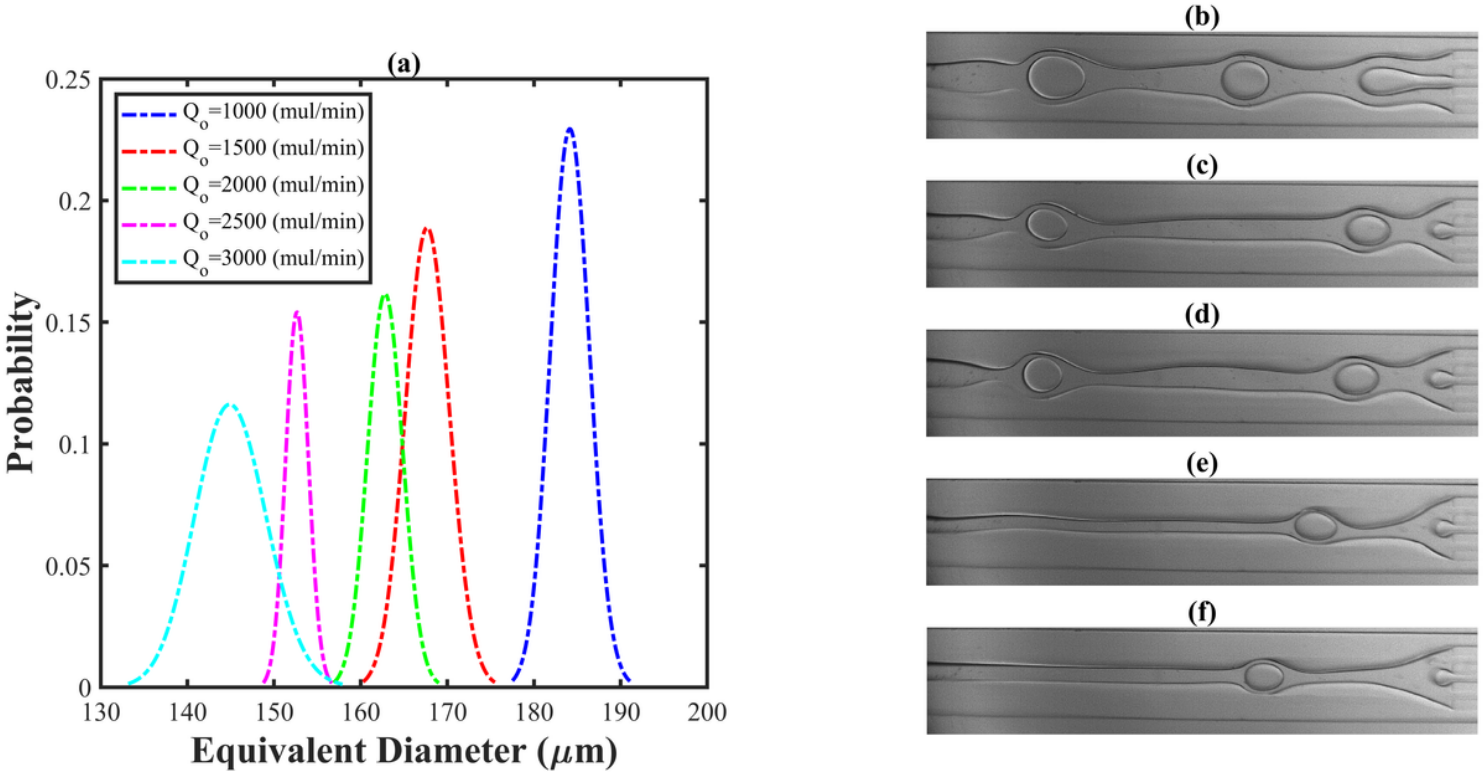

Figure 3

Please see the Manuscript file for the complete figure caption.

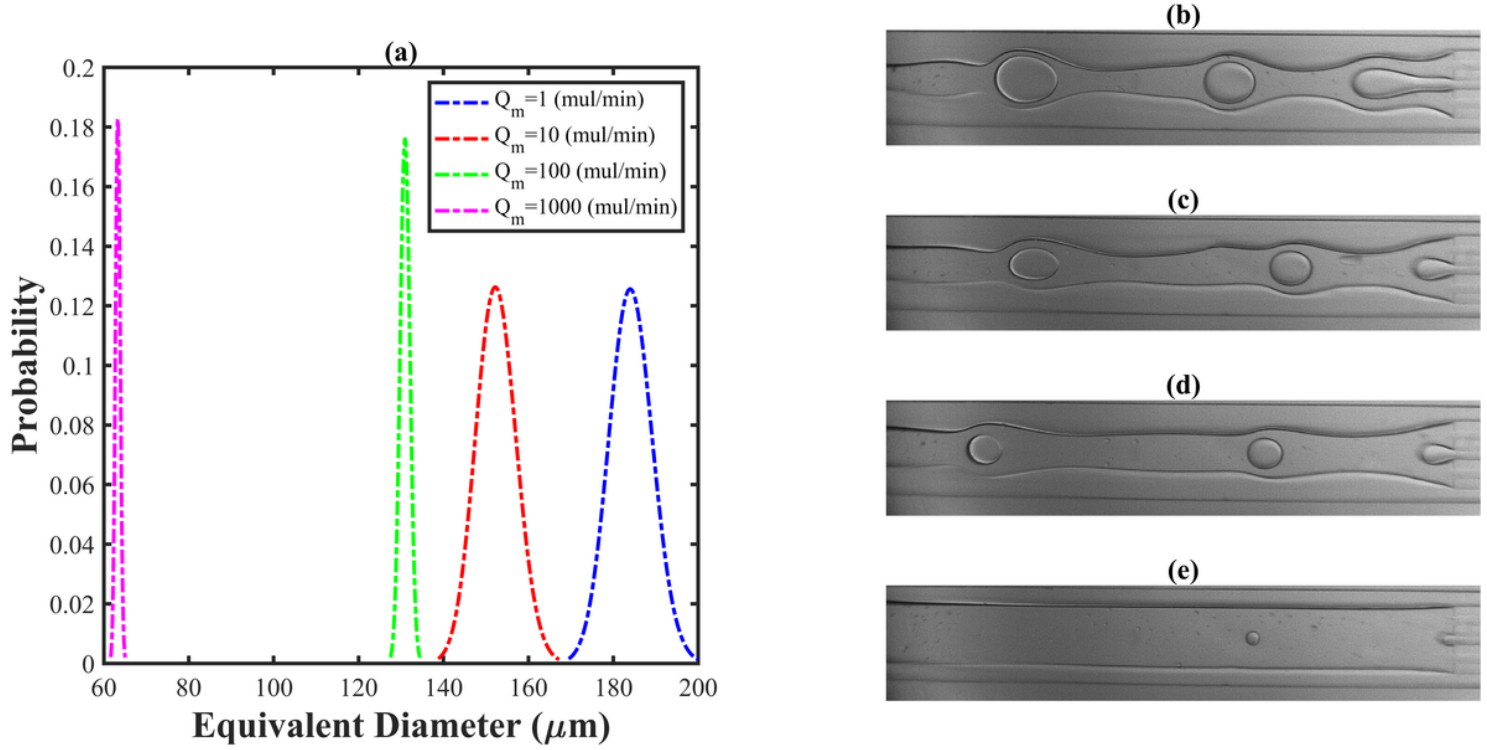

Figure 4

Please see the Manuscript file for the complete figure caption.

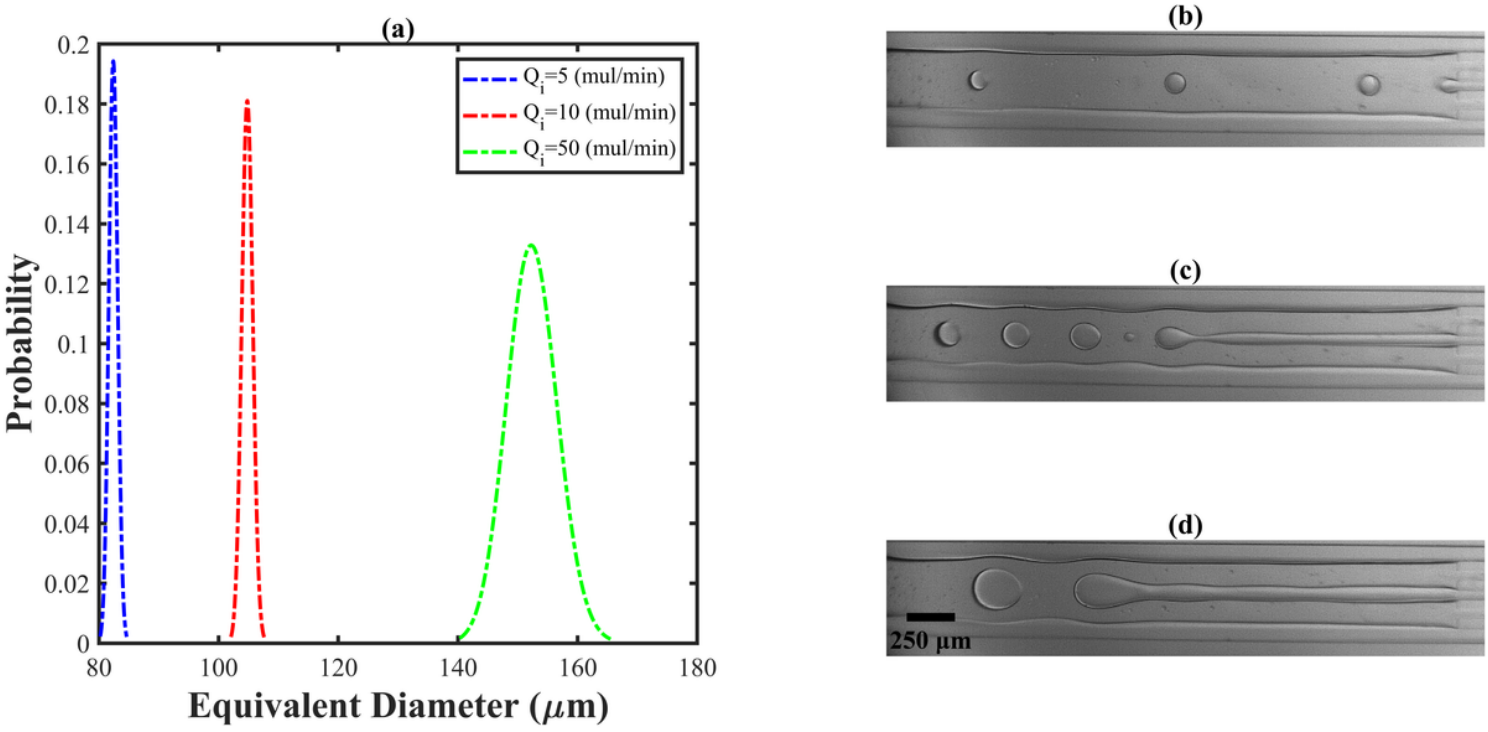

Figure 5

Please see the Manuscript file for the complete figure caption.

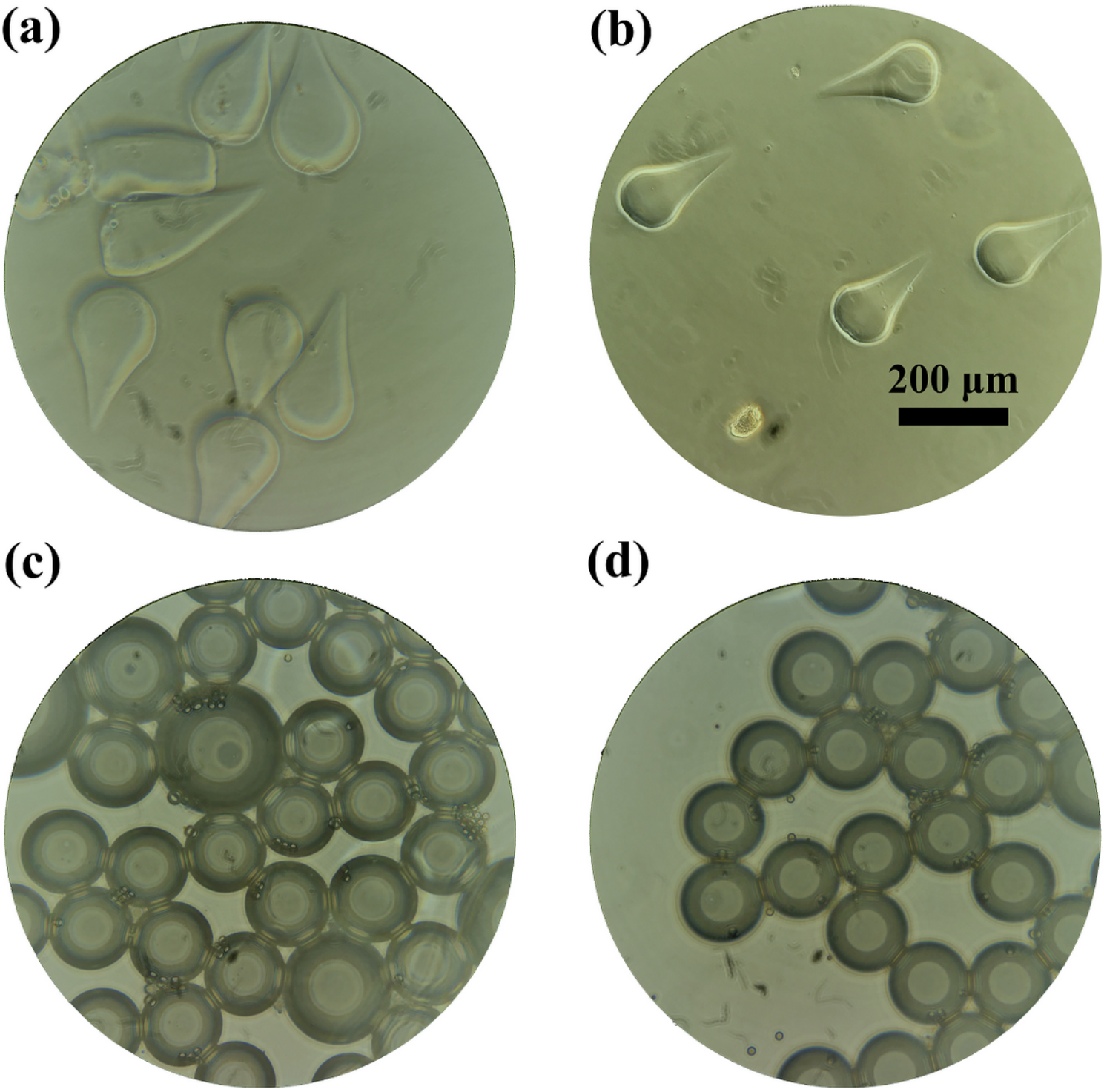

Figure 6

Please see the Manuscript file for the complete figure caption.

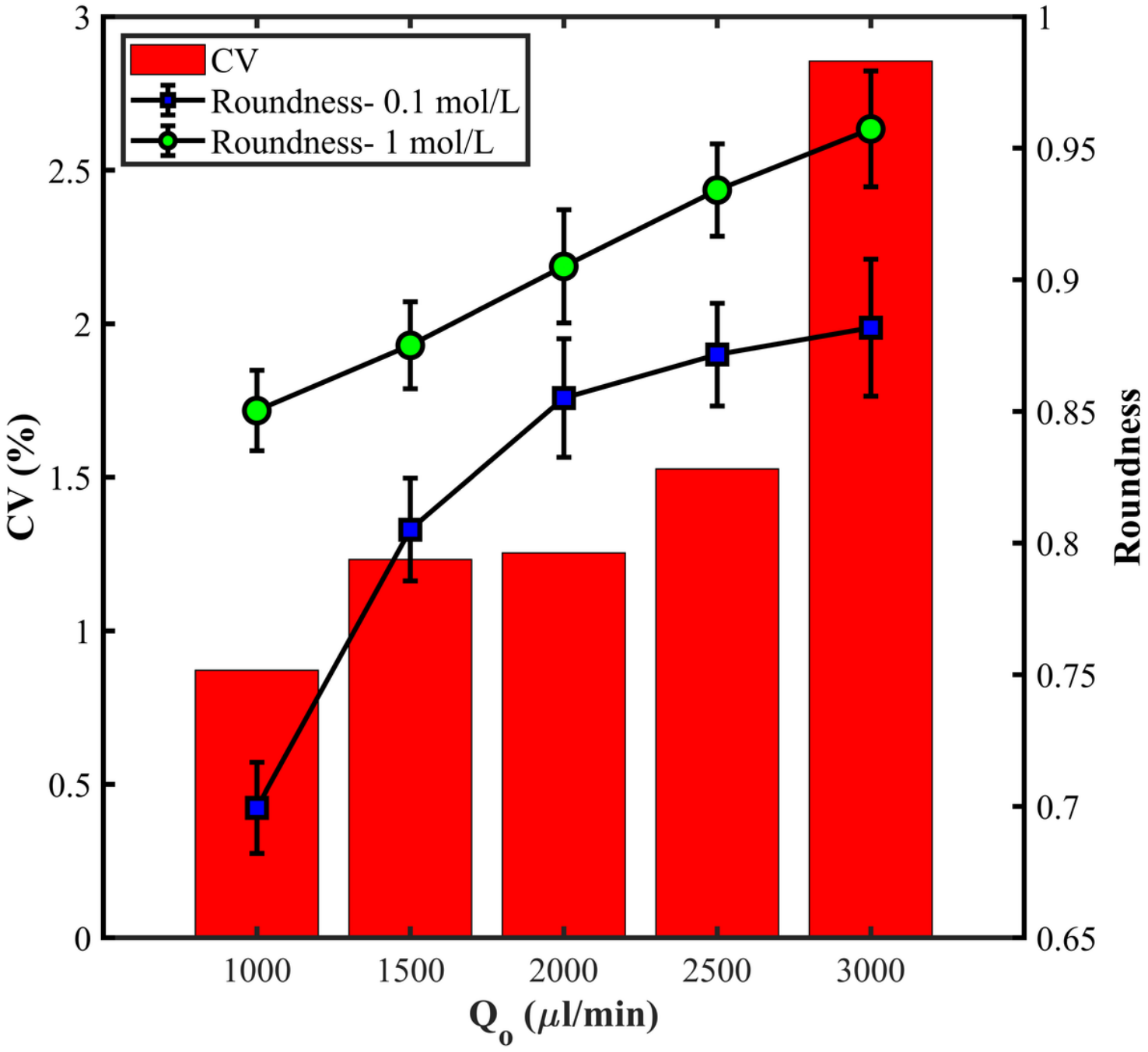

Figure 7

Effect of continuous phase flow rate and calcium chloride concentration on the coefficient of variation and roundness of alginate microgels.